Check for updates

LYMPHOID NEOPLASIA

MLL leukemia induction by genome editing of human CD34$^+$ hematopoietic cells

Corina Buechele,[1] Erin H. Breese,[2] Dominik Schneidawind,[3] Chiou-Hong Lin,[1] Johan Jeong,[1] Jesus Duque-Afonso,[1] Stephen H. K. Wong,[1] Kevin S. Smith,[1] Robert S. Negrin,[3] Matthew Porteus,[4] and Michael L. Cleary[1]

[1]Department of Pathology, [2]Division of Pediatric Hematology/Oncology, Department of Pediatrics, [3]Division of Blood and Marrow Transplantation, Department of Medicine, and [4]Division of Stem Cell Transplantation and Regenerative Medicine, Department of Pediatrics, Stanford University, Stanford, CA

Key Points

- Genome editing of primary human HSPCs generates *MLL* leukemias that model clinical disease features and molecular pathogenesis.

Chromosomal rearrangements involving the mixed-lineage leukemia (*MLL*) gene occur in primary and treatment-related leukemias and confer a poor prognosis. Studies based primarily on mouse models have substantially advanced our understanding of *MLL* leukemia pathogenesis, but often use supraphysiological oncogene expression with uncertain implications for human leukemia. Genome editing using site-specific nucleases provides a powerful new technology for gene modification to potentially model human disease, however, this approach has not been used to re-create acute leukemia in human cells of origin comparable to disease observed in patients. We applied transcription activator-like effector nuclease–mediated genome editing to generate endogenous *MLL-AF9* and *MLL-ENL* oncogenes through insertional mutagenesis in primary human hematopoietic stem and progenitor cells (HSPCs) derived from human umbilical cord blood. Engineered HSPCs displayed altered in vitro growth potentials and induced acute leukemias following transplantation in immunocompromised mice at a mean latency of 16 weeks. The leukemias displayed phenotypic and morphologic similarities with patient leukemia blasts including a subset with mixed phenotype, a distinctive feature seen in clinical disease. The leukemic blasts expressed an *MLL*-associated transcriptional program with elevated levels of crucial *MLL* target genes, displayed heightened sensitivity to DOT1L inhibition, and demonstrated increased oncogenic potential ex vivo and in secondary transplant assays. Thus, genome editing to create endogenous *MLL* oncogenes in primary human HSPCs faithfully models acute *MLL*-rearranged leukemia and provides an experimental platform for prospective studies of leukemia initiation and stem cell biology in a genetic subtype of poor prognosis leukemia. (*Blood*. 2015;126(14):1683-1694)

Introduction

Aberrations of the mixed-lineage leukemia (*MLL*) gene are present in primary and treatment-related acute leukemias of children and adults, and portend an intermediate to poor prognosis. The *MLL* gene encodes a DNA-binding protein that functions as a histone methyltransferase to positively regulate expression of target genes, including multiple *HOX* genes.[1] Its epigenetic role is corrupted by fusions with over 60 different translocation partner proteins in leukemias of various lineages, including acute myeloid leukemia (AML), acute lymphoblastic leukemia (ALL), and a distinctive mixed-phenotype acute leukemia (MPAL).[2-4] Despite their poor prognosis, *MLL* leukemias are genetically simple and appear to require very few additional driver mutations beyond the activated *MLL* oncogene for their pathogenesis, consistent with the short latency between *MLL* gene rearrangements in utero and clinical presentation of leukemia in infants.[5-7] Given their genomic simplicity and short progression, *MLL* leukemias are particularly amenable to experimental modeling for study of their pathogenesis. However, many productive attempts to model this process are based on supraphysiological expression of *MLL* fusion proteins in primary mouse or human cells using retroviral vectors. Unlike human leukemias, these models maintain 2 normal copies of the *MLL* gene and circumvent the endogenous feedback regulation of the fusion gene. Other approaches have simulated MLL oncogenic fusions by creating knock-in mouse models using homologous recombination in embryonic stem cells.[8-10] Although these studies have provided important insights, it remains uncertain whether the experimental models accurately reflect the pathology underlying the disease as it manifests in human patients.

In the past several years, new experimental techniques have been developed to edit the genome in situ for potential correction or modeling of human diseases. These approaches are based on the use of custom DNA nucleases including zinc finger nucleases,[11,12] transcription activator-like effector nucleases (TALENs),[13] and RNA-guided endonucleases of the clustered regularly interspaced

Submitted May 18, 2015; accepted August 23, 2015. Prepublished online as *Blood* First Edition paper, August 26, 2015; DOI 10.1182/blood-2015-05-646398.

The Affymetrix gene expression data reported in this article have been deposited in the Gene Expression Omnibus database (accession number GSE68879).

The online version of this article contains a data supplement.

The publication costs of this article were defrayed in part by page charge payment. Therefore, and solely to indicate this fact, this article is hereby marked "advertisement" in accordance with 18 USC section 1734.

© 2015 by The American Society of Hematology

Downloaded from http://ashpublications.net/blood/article-pdf/126/14/1683/1389098/1683.pdf by guest on 20 May 2024

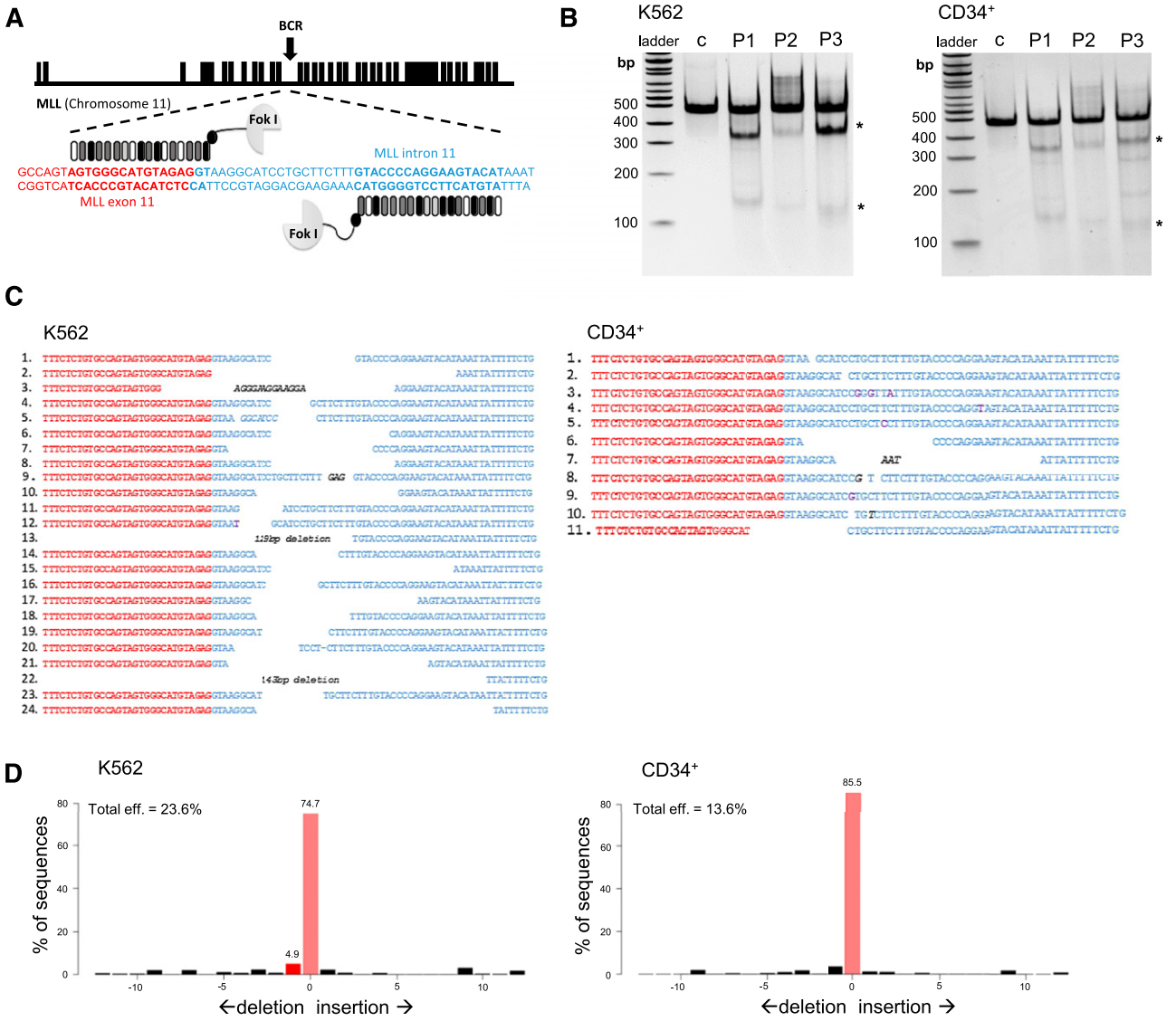

Figure 1. TALENs induce specific DNA DSBs within the *MLL* gene. (A) Schematic illustration of the human *MLL* gene shows recognition sites (bold sequences) for TALEN pairs designed to cleave within the 5′ portion of *MLL* intron 11. Black boxes represent respective exons of the *MLL* gene. (B) Gel image shows results of the T7 endonuclease assay performed on gDNA isolated from K562 or CD34$^+$ cells nucleofected with the 3 different *MLL* TALEN pairs (P1, P2, P3) or control (GFP) as indicated. Digested PCR products (*) of the *MLL* locus represent the presence of strand mismatches resulting from indels that are generated during nonhomologous end joining (NHEJ) repair of DSBs. (C) DNA sequences of the amplified endogenous *MLL* locus resulting from the best TALEN pair (P3) show unique insertions or deletions resulting from NHEJ (K562 24 of 70: 34.3%; CD34$^+$ 11 of 70: 15.7% mutation ratio). Italic letters represent insertions; underlined letters denote TALEN binding sites; red and blue text indicates *MLL* exon 11 and *MLL* intron 11, respectively. (D) Indel frequencies were measured by TIDE and compared with indel frequencies of the control sample.[21] eff., efficiency.

short palindromic repeats[14] that specifically cleave genome target sites to facilitate site-specific mutation or recombination. Genome editing of murine hematopoietic stem and progenitor cells (HSPCs) has been used to generate myeloid malignancy in mice[15] but the approach has not been used to induce acute leukemia in human cells that serve as de novo targets for disease origination in patients. Here, we used TALENs to specifically engineer endogenous activation of 2 common *MLL* oncogenes, *MLL-AF9* and *MLL-ENL*, in primary human HSPCs. Their transplantation in mice led to human leukemias that manifest the pathological and clinical attributes seen in *MLL* leukemia patients.[2-4,16] Our study highlights the application of genome-editing tools in primary human HSPCs to activate oncogenes under the control of the endogenous promoter to faithfully model *MLL*-rearranged leukemias.

Methods

TALEN construction and validation

The *MLL* cleavage site was selected based on the most commonly found patients' breakpoint cluster region (BCR) in the *MLL* gene available through GenBank using the TAL Effector Nucleotide Targeter 2.0.[17,18] Three pairs of TALENs were created using the Golden Gate TALEN Assembly Method.[19] Following nucleofection of the TALEN pairs, genomic DNA (gDNA) was isolated and the targeted region of interest was amplified by polymerase chain reaction (PCR) with *MLL*-specific primers (5′GCCTTTTAATAGTCCGTGTCT3′ and 5′TCTTTAGCTGGTTTAAACAGG3′) and analyzed using the T7 endonuclease assay as previously described.[20]

For sequence analysis of TALEN cut sites, gel-extracted DNA was cloned into the pCR2.1-TOPO vector with the TOPO TA Cloning kit (Invitrogen) and

Downloaded from http://ashpublications.net/blood/article-pdf/126/14/1683/1389098/1683.pdf by guest on 20 May 2024

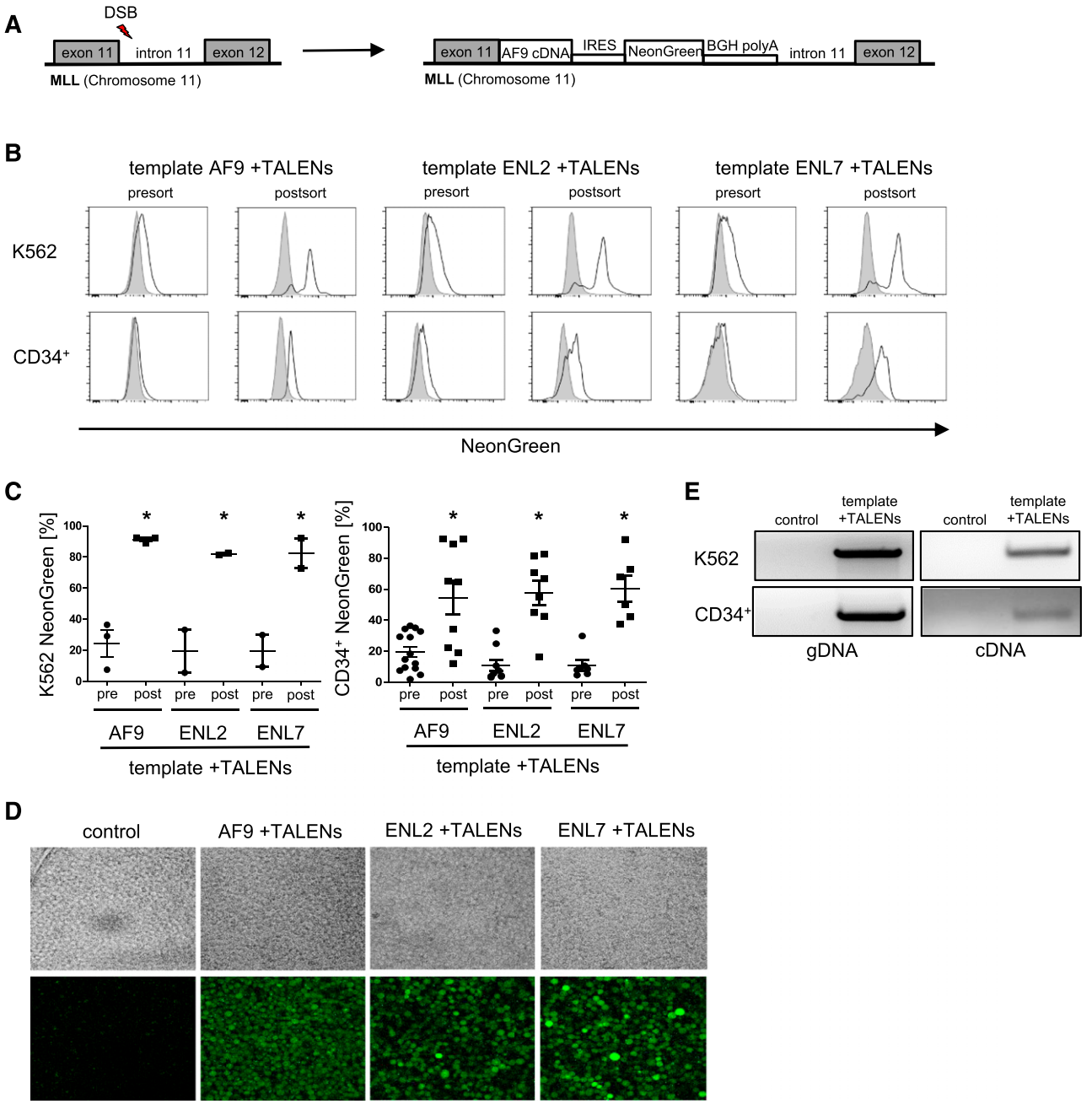

Figure 2. Generation of *MLL-AF9* and *MLL-ENL* knock-in genes by genome engineering. (A) Schematic illustration of experimental strategy to induce a DSB by TALENs followed by integration of the knock-in template in the *MLL* gene locus by homology-directed repair (HDR). (B) FACS profiles show fluorescence of K562 and CD34$^+$ cells nucleofected with the knock-in template alone (gray line) or in combination with the *MLL* TALENs (black line) sorted on days 5 and 3, respectively. (C) Summary of NeonGreen expression in K562 (n[AF9] = 3, n [ENL2/7] = 2) and CD34$^+$ cells (n[AF9] = 11, n[ENL2] = 7, n[ENL7] = 5) pre- and postsort. *$P < .05$ was considered statistically significant. Error bars indicate standard error of the mean (SEM). (D) Confocal microscopy images show NeonGreen expression in sorted K562 and control cells as indicated. Top row, cell density (brightfield); bottom row, NeonGreen expression detected by GFP excitation (450-490 nm) and ×10 objective. (E) PCR/RT-PCR was performed on gDNA and cDNA isolated from NeonGreen-positive K562 and CD34$^+$ cells to detect integration and transcription of the construct under control of the endogenous *MLL* promoter (representative results shown for *MLL-AF9*). BGH, bovine growth hormone.

transformed into competent XL-1 *Escherichia coli* cells. For analyzing allele modification frequencies, the purified PCR products were Sanger-sequenced and each sequence chromatogram was analyzed with the online Tracking of In/dels by Decomposition (TIDE) software (available at http://tide.nki.nl). Analyses were performed using a reference sequence (green fluorescent protein [GFP] sample).[21]

AF9 and *ENL2/7* knock-in construct design

The knock-in DNA templates contained *MLL* homology arms (~700 bp) flanking the TALEN cleavage site, fusion partner complementary DNA (cDNA) sequences, an internal ribosomal entry site (IRES), a fluorescent marker gene coding NeonGreen, and a polyA tail (nucleotide sequences provided in supplemental Figure 1, see supplemental Data available at the *Blood* Web site).[22] The constructs were synthesized commercially (GenScript USA Inc).

Cell culture, nucleofection, and retroviral transduction

K562 cells were cultured and nucleofected as previously described.[20] HSPCs were isolated from fresh human umbilical cord blood (huCB) obtained from the maternity ward of Stanford Hospital (under institutional review board–approved

Downloaded from http://ashpublications.net/blood/article-pdf/126/14/1683/1389098/1683.pdf by guest on 20 May 2024

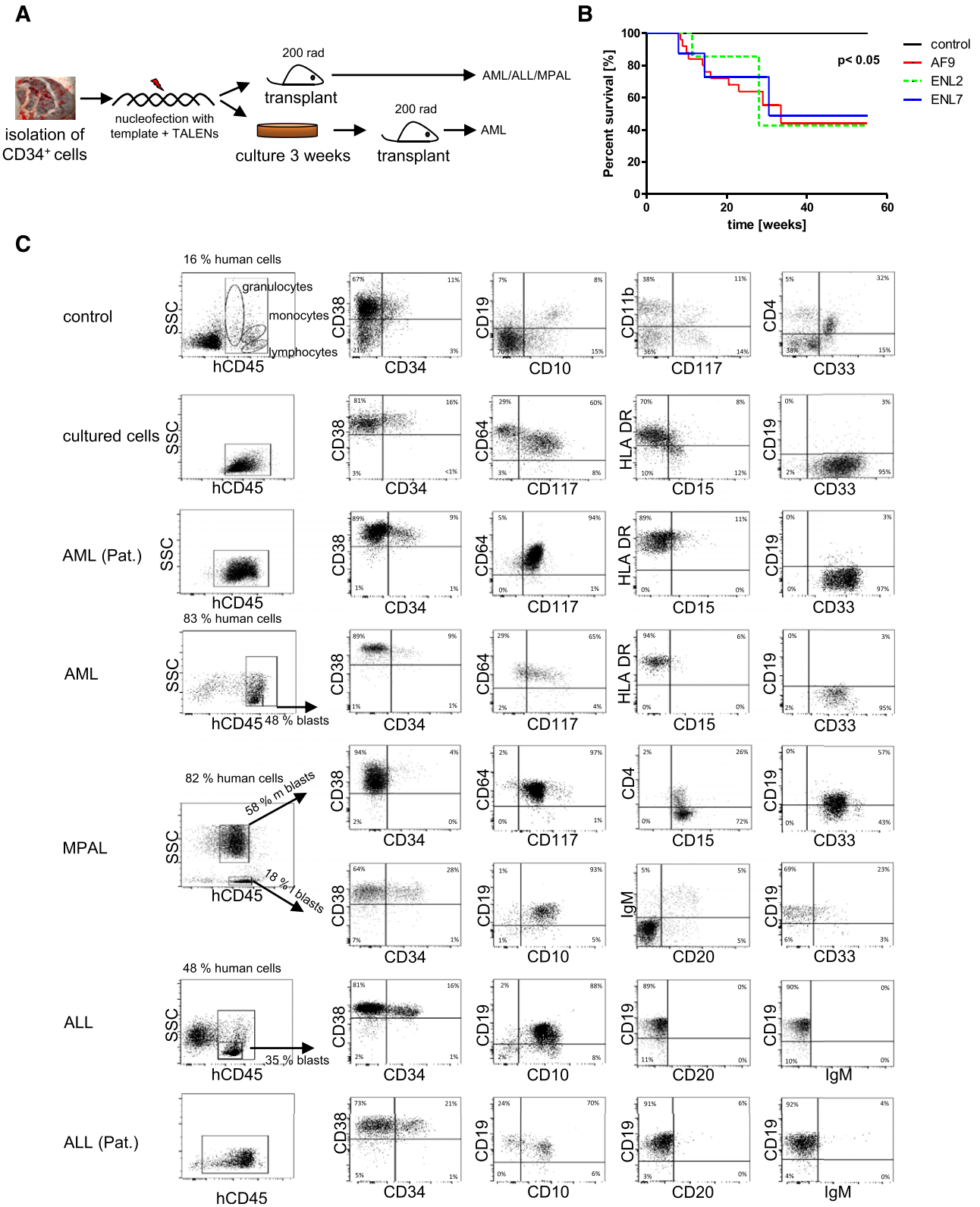

Figure 3. Induction of acute leukemias following transplantation of human CD34$^+$ cells containing knock-in *MLL* oncogenes. (A) Experimental scheme depicts nucleofection of CD34$^+$ cells and their subsequent transplantation directly into sublethally irradiated NSG recipient mice or culture for 3 weeks in vitro prior to transplantation. (B) Kaplan-Meier plot is shown for cohorts of mice transplanted with CD34$^+$ cells transfected with templates plus TALENs (n [AF9] = 25: direct inject = 19, cultured cells = 6; n [ENL2] = 7: direct inject = 5, cultured cells = 2; n [ENL7] = 8: direct inject = 5, cultured cells = 3) or template alone (control, n = 7). $P < .05$ was considered statistically significant. Mice were sacrificed upon signs of illness. (C) Flow cytometry profiles show representative phenotypes of various leukemias that developed in mice transplanted with CD34$^+$ cells (n = 17) compared with blasts from patients with *MLL* translocations (AML/ALL), which display comparable phenotypes. Also shown are representative profiles of BM cells from control mice (n = 2) that received CD34$^+$ cells nucleofected with knock-in construct alone (week 16 posttransplantation) and representative analysis of knock-in cells 3 weeks after cell culture prior to transplantation. l, lymphoid; m, myeloid; (Pat.), patient.

Downloaded from http://ashpublications.net/blood/article-pdf/126/14/1683/1389098/1683.pdf by guest on 20 May 2024

Table 1. Pathological features of leukemias arising in mice transplanted with engineered hCD34$^+$ HSPCs

No.	Oncogene insertion	Cell count prenuc. $\times 10^6$	In vitro culture, days	Latency, weeks	BM hCD45, %	Phenotype	Spleen, mg	Secondary Tx, pos/total inj.
1	AF9	1	21	9	75	AML	20	1/3
2	AF9	1.0	21	14	83	AML	40	0/2
3	AF9	1.5	1	33.5	87	AML	100	nd
4	AF9	1.2	0	14	75	MPAL	50	1/1
5	AF9	2.8	0	16	84	MPAL	40	1/1
6	AF9	3.3	1	20.5	82	MPAL	40	2/4
7	AF9	2.7	0	23	81	MPAL	20	1/1
8	AF9	1.5	0	8.5	90	ALL	180	nd
9	AF9	2.4	0	10	93	ALL	120	1/3
10	AF9	2.2	2	10.5	48	ALL	140	nd
11	AF9	1.5	1	32	77	ALL	70	nd
12	AF9	2	2	29	72	ALL	110	nd
13	ENL2	3	0	11.5	95	ALL	80	2/2
14	ENL2	2.7	0	28	92	ALL	120	nd
15	ENL7	3.6	1	8	90	ALL	80	1/2
16	ENL7	2.7	0	14.5	95	ALL	170	nd
17	ENL7	0.75	1	30.5	82	ALL	30	nd

inj., injected; nd, not determined; pos, positive; prenuc., prenucleofection; Tx, transplantation.

research protocol) using Ficoll-Paque plus (GE Healthcare Life Sciences) followed by the EasySep CD34$^+$ Human Selection kit (StemCell Technologies) to obtain enrichment >90%. Following isolation, CD34$^+$ cells were maintained in serum-free StemSpan II media (StemCell Technologies) supplemented with cytokines (PeproTech: stem cell factor [SCF], thrombopoietin [TPO], Flt3L, interleukin-6 [IL-6], IL-3 [100 ng/mL each]; Cellagen Technology: StemRegenin1 [SR1; 0.75 μM]). The following day, CD34$^+$ cells were nucleofected using the Lonza 4-D Nucleofector system (program EO-100). Cells were incubated at 37°C, 7.5% CO_2 in serum-free media (StemSpan II) + cytokines + 20 μM Z-Vad-FMK (Enzo Life Sciences). After 48 hours, 10% filtered umbilical cord blood plasma was added.

For retroviral transductions, the MLL-AF9 cDNA was cloned into the pMSCV-ires-GFP retroviral vector using standard cloning techniques.[23] Transductions were performed on retronectin-coated (10 μg/mL; Takara Bio Inc) 48-well plastic non-tissue-culture plates that were preloaded with retrovirus by centrifugation at 3000 rpm for 2 hours. CD34$^+$ cells were transduced 2 times on the prepared plates for 4 hours each time at 32°C with freshly loaded retrovirus and transplanted into NSG mice. Explanted leukemia cells were used for further analysis.

CFC assays

CD34$^+$ cells were nucleofected with knock-in constructs without (control) or with MLL TALENs or MLL TALENs alone (control), followed by consecutive fluorescence-activated cell sorting (FACS) for NeonGreen expression at days 2 to 4 of cell culture. On day 21 of liquid culture, cells were seeded in triplicate (10 000 cells per dish) in Methocult H4230 methylcellulose medium (StemCell Technologies) supplemented with SCF, TPO, Flt3L, IL-6, IL-3 (100 ng/mL each) and SR1 (0.75 μM). Colony-forming cell (CFC) assays were performed as previously described.[20,24] Identical conditions were used for CFC assays with explanted leukemic cells from MPAL or AML mice.

Reverse transcription PCR and qPCR

MLL oncogene knock-in was assessed by genomic PCR with the LongAmp Taq PCR kit (New England BioLabs). For each PCR, 200 to 1000 ng of gDNA was used with genomic-specific primers (proof of genomic integration): *MLL* primer: 5′ATCCCTGTAAAACAAAAACCAAAA3′; *AF9* primer: 5′TTGTCATCA GAATGCAGATCTTTC3′, *ENL2* primer: 5′GTACCCCGACTCCTCTACT TTGTA3′, *ENL7* primer: 5′GTAGGTGCCCTTCTTGAGGATCT3′; and for the detection of the wild-type (WT) MLL gene: 5′ACAACTTTGGATGGA AAATAAGGA3′ PCR products were visualized on agarose gel and extracted for Sanger sequencing.

Bone marrow (BM) cells were obtained from the Division of Blood and Marrow Transplantation at Stanford University (under institutional review board–approved research protocol). Mononuclear cells (MNCs) were isolated by using Ficoll-Paque plus and further enriched for B-cell subpopulations by sorting for CD10$^+$CD19$^+$ or CD10$^-$CD19$^+$ cells. RNA was then isolated from MNCs, B-cell subpopulations, or leukemic cells harvested from mice postmortem using the RNeasy Mini kit (Qiagen). RNA was used to generate cDNA using the SuperScript III First-Strand Synthesis System (Invitrogen). PCR was subsequently performed for *MLL* fusion transcripts, *MLL* primer: 5′ATCCCTG TAAAACAAAAACCAAAA3′; *AF9* primer: 5′TTATAGACCTCAAAGGAC CTTGTTG3′; *ENL2* primer: 5′GTACCCCGACTCCTCTACTTTGTA3′; *ENL7* primer: 5′GAAGTCTGAGTCTGAGCTGGAGT3′. PCR products were visualized, gel extracted, and subjected to Sanger sequencing. For detection of target genes *MEIS1* (HS00180020_m1) and *HOXA9* (HS00365956_m1) by quantitative PCR (qPCR), TaqMan gene expression assays were used (Life Technologies). qPCR was performed in triplicate followed by melting curve analysis in the Bio-Rad CFX384 C1000 real-time system relative to Kasumi-1 cells or leukemic BM cells. Results were normalized to the housekeeping gene *ACTB*.

Confocal microscopy

K562 cells were nucleofected with TALENs and the knock-in constructs followed by consecutive FACS for NeonGreen expression at days 5 and 8 of cell culture. Confocal microscopy was performed using a Zeiss LSM 710 confocal scope. A 10× objective and a GFP laser with the excitation 450 to 490 nm were used for the detection of NeonGreen-expressing cells.

DOT1L inhibitor treatment

EPZ00477 (Millipore) was prepared in stock solutions with dimethylsulfoxide (DMSO). CFC assays were performed with cell lines and leukemic cells explanted from MPAL and AML mice as described above (CFC assays) with the addition of increasing EPZ00477 concentrations. After 12 to 14 days, CFC assays were diluted and cell count, CD14, *MEIS1*, and *HOXA9* expression was determined.

Microarray data analysis

BM cells (sorted for human CD45 [hCD45]) of leukemic mice (ALL) were used for global gene expression measurement using the Affymetrix Microarray GeneChip platform (HG-U133 Plus 2.0). The data, together with those from 70 MLL patients (ALL) and 6 control samples (same GeneChip platform) from the leukemia study group, were used for unsupervised hierarchical clustering analysis.[16] The gene expression matrix from the arrays was normalized in the

Downloaded from http://ashpublications.net/blood/article-pdf/126/14/1683/1389098/1683.pdf by guest on 20 May 2024

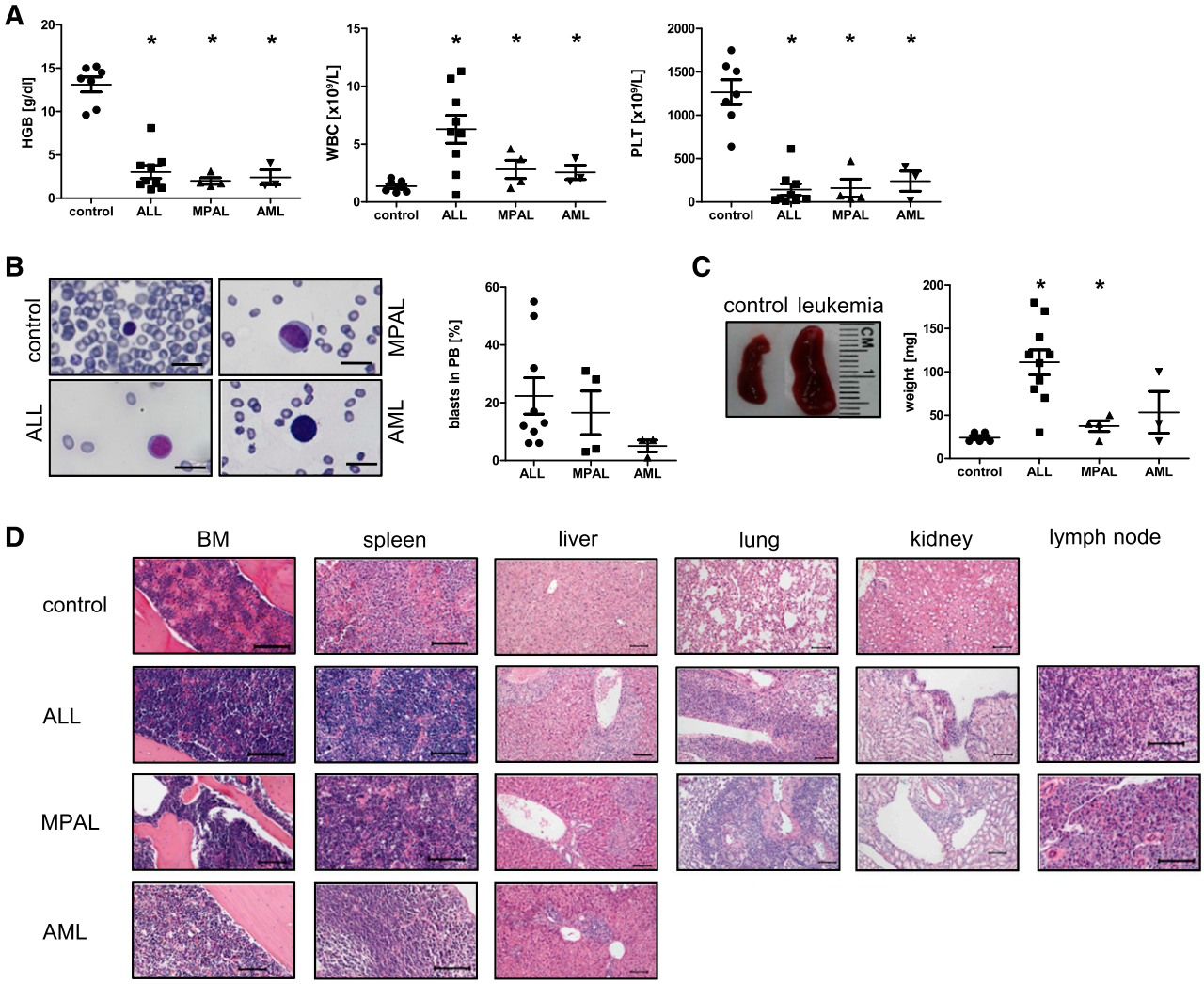

Figure 4. Pathologic and molecular features of acute leukemias induced by genome editing of the *MLL* oncogene. (A) Plots show results of hematologic analyses performed on control (n = 7) and leukemic mice (n = 16), respectively. (B) Representative peripheral blood smears of control and leukemic mice are shown and summarized by calculating the percentage of blast cells (n = 16). Scale bars define 10 μm. (C) Spleen size and weight are shown for 1 representative control and leukemic mice (n = 17). (D) Hematoxylin-and-eosin–stained paraffin sections demonstrate disruption of organ architecture due to tumor infiltration compared with control mice. Scale bars define 100 μm. (E) PCR/RT-PCR was performed on gDNA and cDNA of leukemia cells to detect integration and expression of the *MLL* oncogenes and WT *MLL* gene. (F) Representative western blot analysis shows WT MLL^N and MLL-AF9 expression in control ($CD34^+$ cells nucleofected with template alone) and explanted blast cells from xenotransplants induced by either retroviral transduction or under the expression of the endogenous promoter (MPAL, AML). Glyceraldehyde-3-phosphate dehydrogenase (GAPDH), loading control. Bottom, relative MLL-AF9 band intensities compared with WT MLL^N. (G) Representative qPCR analyses show elevated expression levels of *MLL* target genes compared with non-*MLL* leukemic cell lines or controls (human BM or BM $CD10^{+/-}/CD19^+$) but similar to cell lines and patients with *MLL* translocations. Representative results from 8 independent experiments are shown. (H) Unsupervised hierarchical cluster analysis of 3 leukemic mice (ALL) and 70 *MLL*-rearranged ALL patients showing similar gene expression profiling in contrast to control samples. Each dot (A-C) represents a mouse; horizontal bars represent the mean. $^*P < .05$ was considered statistically significant. Error bars indicate SEM. HGB, hemoglobin; PB, peripheral blood; PLT, platelet; WBC, white blood cell.

same way using the RMA model from Bioconductor affy package. Gene expression values were then independently filtered to remove low-variance probes using the Bioconductor package, genefilter 1.50. Finally, 25 000 probes were then subjected to unsupervised hierarchical clustering analysis using R packages, ape, and heatmap 2.0.

Results

Generation of site-specific DNA DSBs in the *MLL* gene using TALENs

TALENs were designed to introduce DNA breaks at a preselected site at the intersection of exon 11 and intron 11 of the *MLL* gene (Figure 1A). Intron 11 contains a BCR that harbors common sites of chromosomal translocations in patients with *MLL-AF9* or *MLL-ENL* leukemias.[17] To test their abilities to specifically cleave the *MLL* gene, pairs of TALENs were nucleofected into K562 and $CD34^+$ cells and resultant double-strand breaks (DSBs) from the different TALEN pairs were detected using the surveyor assay (Figure 1B).[25] Specific cleavage activity was further assessed by cloning and sequence analyses of target site DNA, which showed unique deletions and insertions in the repaired cutting sites of the TALENs (K562, 34.3%; $CD34^+$, 15.7%) in the cloned fragments (Figure 1C). Additionally, we quantified allele modification frequencies using TIDE analysis (Figure 1D).[21] The *MLL* TALEN pair most efficient at cleavage was used in subsequent experiments to target a DNA DSB at the preselected genomic site of the *MLL* gene in primary cells.

Downloaded from http://ashpublications.net/blood/article-pdf/126/14/1683/1389098/1683.pdf by guest on 20 May 2024

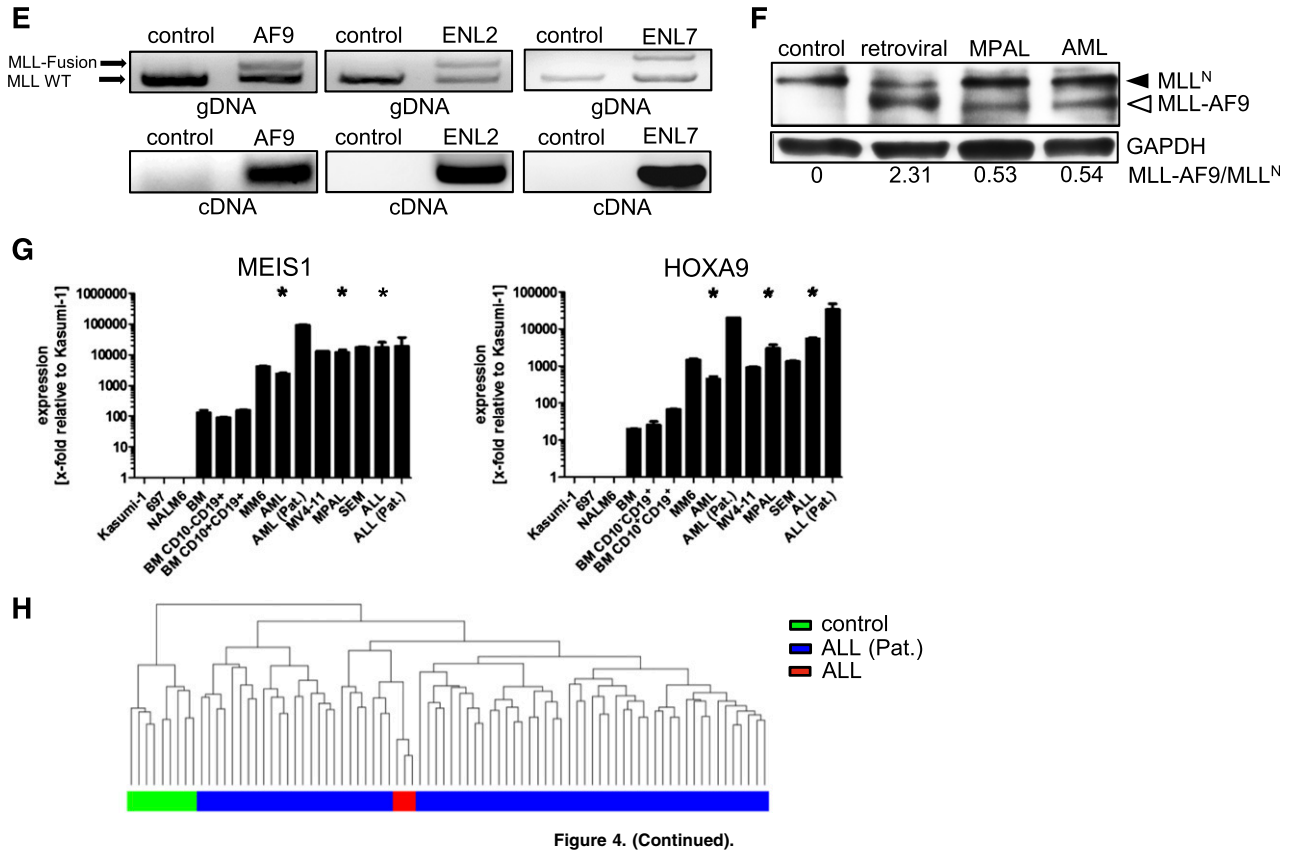

Figure 4. (Continued).

Creation of endogenous *MLL* oncogenes in CD34$^+$ human cord blood cells by genome editing

To promote genome editing at the targeted cleavage site during homology-directed repair,[26] exogenous DNA templates were designed with flanking sequences homologous to the nuclease target site (supplemental Figure 1). Three different templates were designed for insertion of either *AF9* (exon 5-9), *ENL2* (exon 2-12), or *ENL7* (exon 7-12) sequences to create the respective fusion oncogenes expressed under control of the endogenous *MLL* promoter along with the fluorescent marker gene NeonGreen (Figure 2A).[22] The *AF9* construct represented the most common fusion seen in *MLL-AF9* patients.[17,27,28] The *ENL* constructs contained different lengths of the *ENL* cDNA accounting for the majority of *MLL-ENL* fusions seen in patients associated with either ALL or AML.[29-31]

Cotransfection of *MLL* TALENs with the respective knock-in templates resulted in insertions both in K562 cells and in primary HSPCs isolated from huCB with knock-in efficiencies of ~22% (range, 6%-36%) and ~9% (range, 2%-35%), respectively, based on NeonGreen expression, which could be further enriched by FACS (Figure 2B-C). NeonGreen expression in nucleofected cells was also demonstrated by confocal microscopy (Figure 2D). PCR analyses of sorted NeonGreen-expressing K562 and primary CD34$^+$ cells confirmed correct integration and expression of the constructs (Figure 2E). These studies demonstrate that TALENs promote homology-directed insertional mutagenesis to create endogenous *MLL* oncogenes in cell lines and primary human HSPCs.

Insertional activation of endogenous *MLL* oncogenes alters the growth and survival of primary CD34$^+$ cells

To assess the effects of activating an endogenous *MLL* oncogene in primary HSPCs, human CD34$^+$ cells were nucleofected with *MLL* TALENs and knock-in templates or template alone (control). In liquid culture, the engineered CD34$^+$ cells displayed a distinct survival advantage and proliferated for ~100 to 120 days whereas control samples terminally differentiated and eventually died out after 60 to 80 days (supplemental Figure 2A-B).

CFC assays were performed to further assess the clonal expansion capacity and transformative potential of the knock-in cells. For this purpose, 10 000 sorted knock-in or control cells (harvested on day 21 of liquid culture) were plated in semisolid medium. Both populations generated colonies after 10 to 14 days, but the knock-in cells displayed a significantly higher clonogenic potential after the second round of replating as compared with control cells (supplemental Figure 3A). Knock-in cells also demonstrated more compact colony morphologies in contrast to the controls, consistent with more immature cells (supplemental Figure 3B).[24] Despite their enhanced growth properties, knock-in cells were not fully transformed because further replating resulted in decreasing cell numbers consistent with the proliferative exhaustion observed in extended liquid cultures.

CD34$^+$ cells engineered to express *MLL* oncogenes induce acute leukemias

CD34$^+$ huCB cells were cotransfected with *MLL* TALENs and the knock-in constructs, and were then transplanted using 2 alternative approaches: unsorted nucleofected cells were either injected directly (<3 days) into NSG immunocompromised mice or cultured in vitro (3 weeks) under myeloid growth conditions prior to transplantation (Figure 3A). IV injection of uncultured CD34$^+$ HSPCs (0.75-3.6 $\times$ 10^6, median 2 $\times$ 10^6 CD34$^+$ cells) or cultured cells (1 $\times$ 10^6) induced acute leukemia within 8 to 33.5 weeks (median 16 weeks) posttransplantation (Figure 3B). *MLL-AF9* knock-in cells induced ALL, MPAL, or AML,

Downloaded from http://ashpublications.net/blood/article-pdf/126/14/1683/1389098/1683.pdf by guest on 20 May 2024

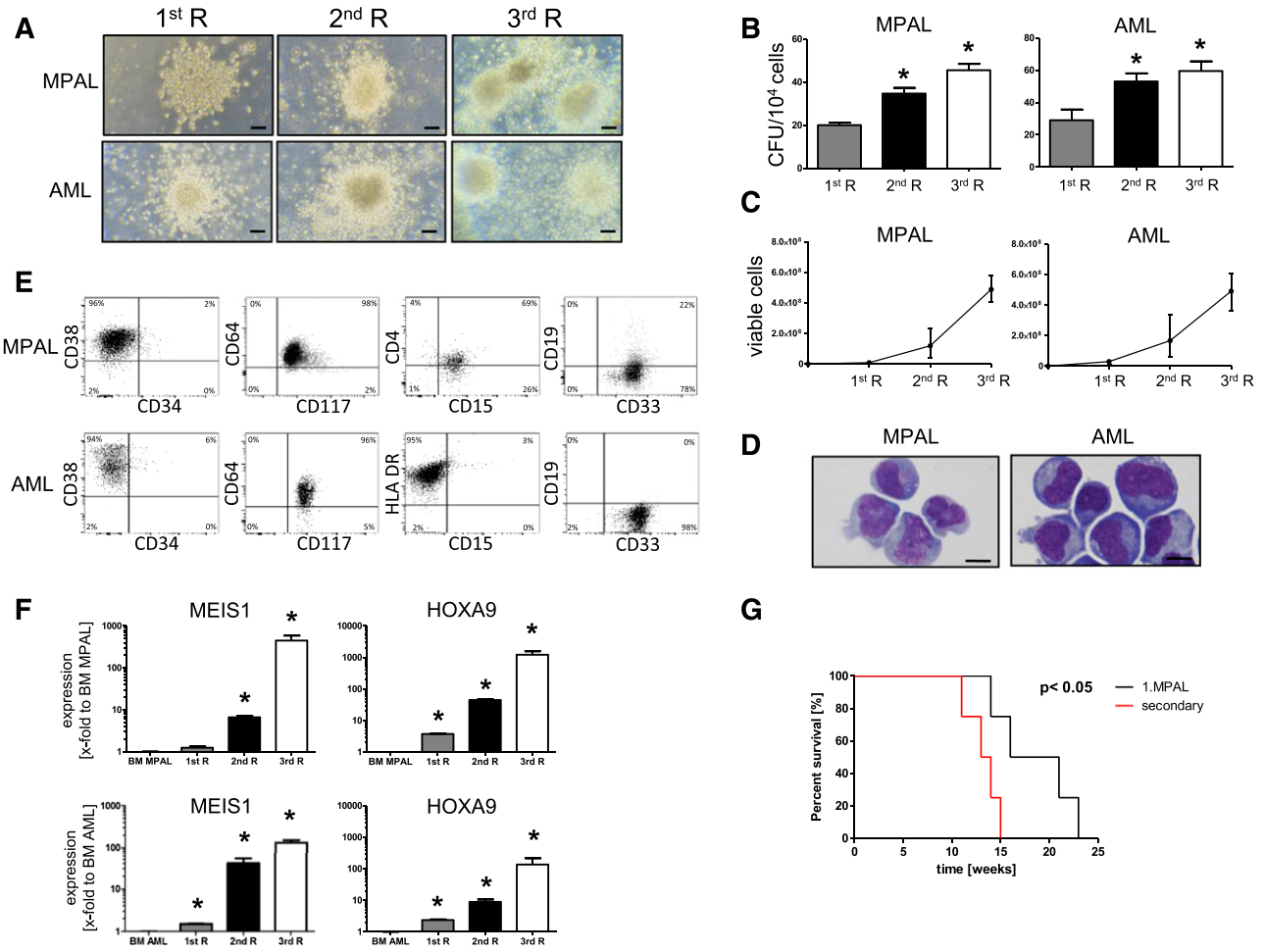

Figure 5. Immortalization ex vivo and increased oncogenic potential through CFC assays of *MLL* edited acute leukemia cells. CFC assays were performed to assess the replating efficiency of leukemic cells ex vivo in semisolid medium. Scale bars define 100 μm. (A) Images show representative morphologies of compact colonies displaying increased density after each replating. (B) Bar graph represents the mean number of colonies generated per 10^4 seeded cells. (C) Plot indicates cell numbers after each replating. Pooled data from 3 independent experiments. (D) Representative morphologies and phenotypes (E) are shown for colony-forming cells. Scale bar defines 10 μm. (F) Representative qPCR analyses of *MLL* target genes show increasing levels after each replating in CFC assays. Results from 1 of 3 independent experiments performed in triplicate. (G) Kaplan-Meier plot is shown for each cohort of animals (direct inject = 4 and secondary inject = 4). $^*P < .05$ was considered statistically significant. Error bars indicate SEM. CFU, colony-forming unit; R, round.

whereas the *ENL* knock-in cells exclusively resulted in an ALL phenotype (Table 1). Mice transplanted with control cells (nucleofected with template alone, hereafter referred to as control mice) displayed no overt pathology. Rather, periodic BM aspirations showed an initial lymphoid engraftment in the control mice, which subsequently developed additional features of myeloid hematopoiesis with evidence of terminal differentiation characterized by increased expression levels of CD38. Control mice presented with common gates for lymphocytes, monocytes, and granulocytes detected by different CD45 expression levels and side-scatter (SSC) profiles (Figure 3C first row, 16 weeks postinjection).

Leukemic mice transplanted with *MLL* oncogene knock-in cells presented with typical blasts characterized by a lower expression of hCD45 and distinct SSC characteristics. Different surface phenotypes (ALL, AML, MPAL) of blast cells showed similarities to patient samples harboring *MLL* translocations (Figure 3C rows 3 and 8). The majority of leukemic mice (10 of 17) directly injected with nucleofected cells developed ALL displaying a prelymphoid phenotype with $CD10^+$/$CD19^+$/$CD38^+$/$CD34^+$ and very low expression levels of mature B-cell markers CD20 and immunoglobulin M (IgM) (Figure 3C rows 6 and 7). In some cases, MPAL was observed with immunophenotypic features of AML and ALL in the same recipient mouse (Figure 3C rows 5 and 6). Two distinct blast populations were clearly distinguished by their SSC properties. The ALL cells were phenotypically similar to those in pure ALLs (Figure 3C row 7), whereas a separate blast cell subpopulation displayed a myelomonocytic phenotype ($CD38^+$/$CD33^+$/$CD15^+$/$CD64^+$/$CD4^+$/$CD117^+$) (Figure 3C row 5). Furthermore, coexpression of myeloid and lymphoid antigens was observed on both blast populations.

Short-term in vitro culture (3 weeks) of knock-in cells under myeloid conditions prior to transplantation resulted in AML ($CD38^+$/$CD33^+$/HLA DR^+/$CD64^+$/$CD117^+$) with a median latency of ~12 weeks (Figure 3C row 4). The cultured cells at the time of transplant and their corresponding leukemias displayed similar immature myelomonocytic phenotypes (Figure 3C second row) consistent with a pivotal role of the microenvironment for the lineage determination of *MLL* leukemias.[32,33] Conversely, prolonged (>3 months) antecedent in vitro culture of nucleofected cells prior to transplantation resulted in no engraftment, indicating that knock-in cells did not maintain oncogenic potential in vitro consistent with their differentiation and exhaustion observed in extended in vitro cultures and serial replating CFC assays.

Downloaded from http://ashpublications.net/blood/article-pdf/126/14/1683/1389098/1683.pdf by guest on 20 May 2024

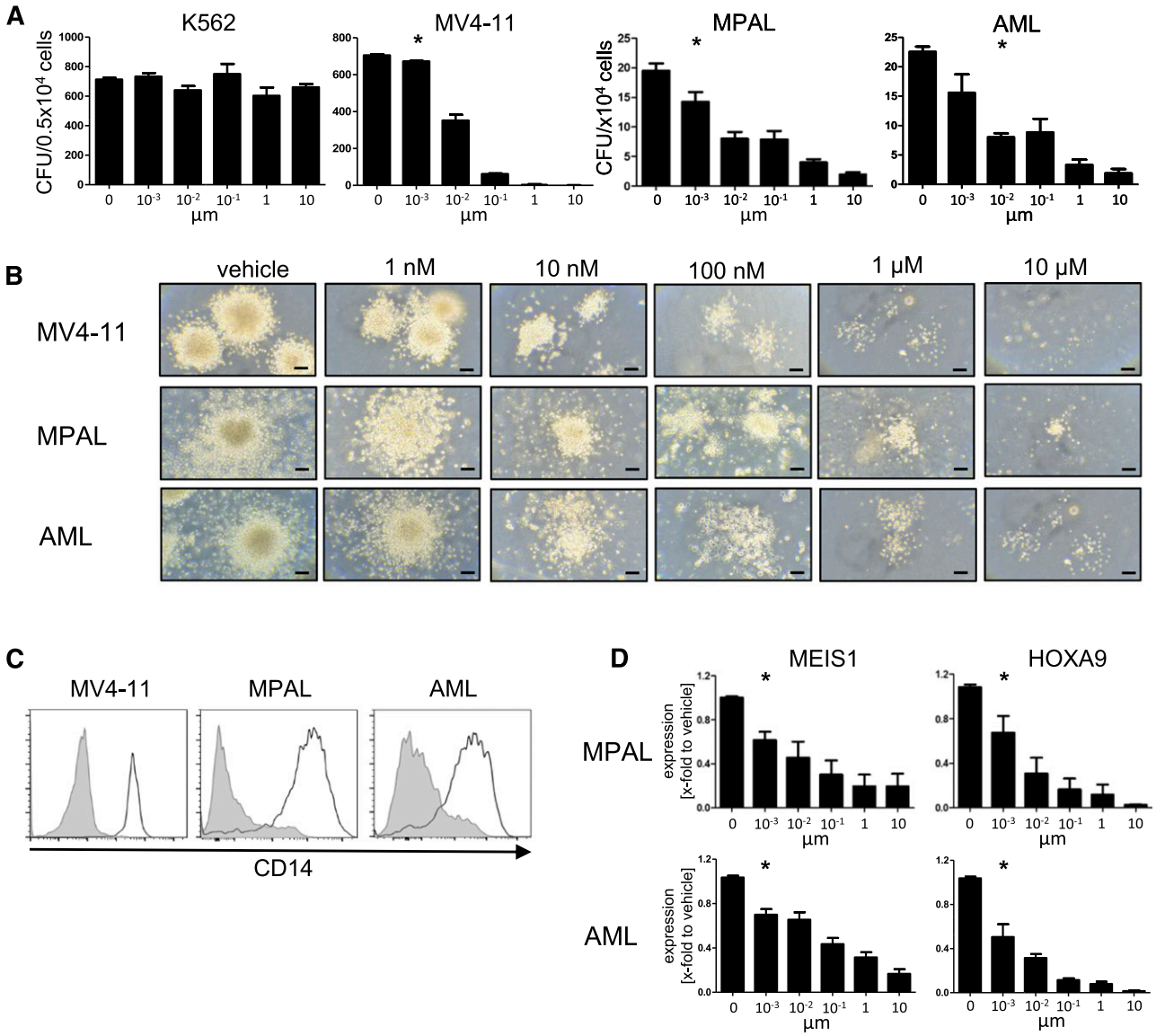

Figure 6. Edited leukemia cells display increased sensitivity to DOT1L inhibition. (A) Bar graph represents the mean number of colonies generated per 5000 or 10^4 seeded cells after 12 to 14 days in the presence of increasing concentrations of EPZ004777 or vehicle (DMSO). Data from 4 (MPAL) and 3 (AML) independent experiments performed in duplicate were pooled together (IC_{50} values: MV4-11, 10 nM; MPAL/AML, 51/11 nM; K562, >50 μM). (B) Images show representative morphologies of colonies displaying decreased density after drug treatment. Scale bars define 100 μm. (C) MV4-11 and leukemic cells (n [MPAL] = 4; n [AML] = 3) were analyzed by flow cytometry for cell surface expression of CD14 after incubation with 10 μM EPZ04777 (black line) or DMSO (gray line) in CFC assays. (D) Representative qPCR analyses of *MLL* target genes show decreasing levels relative to DMSO treatment. Shown are representative data from 1 of 4 (MPAL) and 3 (AML) independent experiments. *$P < .05$ was considered statistically significant. Error bars indicate SEM.

Genome editing of CD34$^+$ cells models human leukemia in mice

All mice that succumbed to fatal leukemia presented with a similar disease profile that included anemia, leukocytosis, and thrombocytopenia (Figure 4A) and blasts in peripheral blood (Figure 4B). Splenomegaly was most prominent in ALL mice (Figure 4C). Histopathological examination confirmed extensive replacement of BM and infiltration of the spleen, liver, and other peripheral organs (Figure 4D) by leukemic blasts that expressed the respective oncogenes and normal WT *MLL* gene detected by PCR, reverse transcription PCR (RT-PCR), and western blot (Figure 4E-F). The expression level under control of the endogenous promoter was lower compared with that in AMLs induced by ectopic expression of MLL-AF9 by retroviral transduction of huCB cells.[23] Cytospins showed monomorphic immature blast cells (supplemental Figure 4). Moreover, the leukemic blasts demonstrated increased expression levels of common *MLL* target genes (*MEIS1*, *HOXA9*) compared with human BM cells or non-*MLL* leukemic cell lines and similar to *MLL* rearranged cell lines (Mono Mac 6 or MV4-11) and patient samples harboring *MLL* translocations (Figure 4G). Furthermore, gene expression profiling of *MLL-AF9*– or *MLL-ENL*–expressing blast cells demonstrated a signature that closely parallels that of publicly available patient samples harboring an *MLL* rearrangement (Figure 4H).[16] These studies establish a novel experimental model to generate *MLL* leukemias deriving from primary human HSPCs expressing the fusion oncogene under control of the endogenous promoter.

Leukemic cells explant, proliferate ex vivo, and serial transplant with enhanced oncogenic potential

Leukemic blast cells were explanted from MPAL and AML mice into serial CFC assays where they formed predominantly compact colonies (Figure 5A), which increased in number and total cell

Downloaded from http://ashpublications.net/blood/article-pdf/126/14/1683/1389098/1683.pdf by guest on 20 May 2024

counts after each serial replating (Figure 5B-C). The cellular morphology and phenotypes were comparable to the AML blast portion present in leukemic mice (Figure 5D-E). Cultured cells demonstrated significantly increased expression of *MLL* target genes *MEIS1* and *HOXA9* after each replating, suggesting expansion and enrichment for leukemia-propagating cells in vitro (Figure 5F). The explanted cells displayed indefinite growth ex vivo in contrast to the limited in vitro growth potentials of fresh knock-in cells that eventually exhausted during sequential replatings. The CFCs were serially transplanted into secondary recipients, which showed an analogous pathologic phenotype as primary recipients except that the median latency of secondary disease was significantly shorter than the primary leukemias, and only the AML blast portion was present after culturing them under myeloid growth conditions in CFC assays (Figure 5G). The more robust oncogenic properties of leukemic cells vs fresh nucleofected cells suggest that activation of the *MLL* oncogene alone did not fully transform human HSPCs, which must acquire additional transformation events in vivo to advance to acute leukemia.

Gene-edited leukemias display increased sensitivity to DOT1L inhibition

DOT1L catalyzes the methylation of H3K79, a chromatin modification that leads to enhanced expression of leukemogenic genes, including *HOXA9* and *MEIS1* in *MLL*-rearranged leukemias.[34-44] Small-molecule inhibitors of DOT1L have been developed and are currently undergoing phase 1 clinical trials.[45-50] We tested leukemic blast cells explanted from MPAL and AML mice for sensitivity to the DOT1L inhibitor EPZ004777 in comparison with the human *MLL*-rearranged leukemia cell line MV4-11 and non-*MLL*-rearranged K562 cells. In CFC assays, the explanted blasts and MV4-11 cells displayed high sensitivity to EPZ004777 in a dose-dependent manner characterized by a decrease of colony number and size, whereas K562 cells showed no significant differences (Figure 6A-B). EPZ004777 induced differentiation of leukemic and MV4-11 cells characterized by the induction and increased expression of CD14 (Figure 6C). The compound also inhibited expression of target genes, *HOXA9* and *MEIS1*, in the *MLL* leukemic cells (Figure 6D). These data demonstrate the dependence of gene-edited leukemias on DOT1L, a signature feature of primary acute *MLL*-rearranged leukemias.

Discussion

Using genome-editing techniques, we generated *MLL-AF9* and *MLL-ENL* oncogenes in primary human HSPCs based on knock-in mutations of the endogenous *MLL* gene to model the consequences of oncogene activation in human leukemia both in vitro and in vivo using a huCB xenotransplantation assay. Our studies demonstrate that the $CD34^+$ fraction of huCB cells is capable of initiating leukemia in response to endogenous activated *MLL-AF9* or *MLL-ENL* oncogenes. The productive insertion of knock-in constructs under control of the endogenous *MLL* promoter was confirmed by the expression of a NeonGreen marker gene by flow cytometry, confocal microscopy, and PCR. Two alternative transplantation approaches differed with respect to whether knock-in cells were subjected to antecedent culture prior to transplantation in NSG mice. Culture in vitro (3 weeks) under myeloid growth conditions prior to transplantation resulted in AML, whereas direct injection (<3 day of in vitro culture) led to the development of ALL, AML, or MPAL induced by *MLL-AF9* oncogene expression, or ALL induced by *MLL-ENL* constructs. Although limited by overall cohort sizes, our data support and are consistent with previous reports showing that both microenvironmental cues and the fusion partner serve primary roles in lineage determination of leukemia.[32,33]

Although previous studies utilizing a variety of in vivo models have substantially advanced our understanding of *MLL* leukemia pathogenesis,[32,33,51-53] they may not fully reconstitute leukemia as it manifests in human patients. For example, genetically engineered mouse models driven by germline or somatic *MLL* oncogene activation may be limited by species-specific differences in genetic background and requirements for leukemic transformation.[8-10] Retroviral transduction/transplantation models using mouse HSPCs are widely used but may not accurately recapitulate the role of *MLL* fusion proteins in human diseases.[23,54] Xenotransplantation studies using transduced primary human cells offer a potentially more relevant approach for modeling leukemia pathogenesis, but suffer from limitations of nonphysiological oncogene expression under control of the retroviral long terminal repeat, which is more broadly expressed and resistant to differentiation-linked downregulation compared with the endogenous *MLL* promoter. Furthermore, retroviral models maintain the presence of 2 wild-type *MLL* genes. Therefore, it remains uncertain to what extent these models mirror the naturally occurring disease in humans.

The genome-editing approach developed in our studies bypasses these limitations and provides a novel method to explore the roles of various initiating events in leukemia pathogenesis de novo in a prospective, physiologic, and faithful manner using primary human HSPCs. Notably, activation of endogenous *MLL* oncogenes in human HSPCs induced transient enhancement of in vitro growth potentials, but the effects were not as strong as those observed in retroviral transduction of both primary murine and human HSPCs, which display unlimited growth potentials in methylcellulose assays.[23,33] Thus, previous models may actually induce more robust oncogenic readouts than the genomic aberrations that activate the endogenous *MLL* gene in primary human HSPCs.

huCB leukemias generated by our approach faithfully recapitulate many features of the clinical disease present in a subset of leukemia patients associated with *MLL* chromosomal translocations. They are consistent with the original designation of *MLL* as the mixed lineage leukemia oncogene.[55] Moreover, the phenotype, morphology, and molecular features of the induced leukemias presented in our study are similar to patient leukemic blasts. This includes expression of an *MLL*-associated transcriptional program with elevated levels of crucial *MLL* target genes *HOXA9* and *MEIS1*, which have well-described roles in both the induction and maintenance of *MLL*-fusion leukemias.[56-58] Similar to clinical observations, the leukemias displayed heightened sensitivity to DOT1L inhibition consistent with aberrant recruitment and dependence on this histone methyltransferase in leukemias driven by *MLL-AF9* and *MLL-ENL* oncogenes and could serve for drug screening of human cells.

In the present study, the development of leukemia was relatively rapid, with a median latency of 16 weeks. Although expression of MLL-AF9 or MLL-ENL is the primary genetic defect responsible for the defining characteristics of disease, MLL fusion alone was not sufficient to drive unlimited proliferation of human HSPCs in our cultures compared with the more robust growth of explanted leukemia cells consistent with the acquisition of additional genetic or epigenetic events in vivo. The rapid progression of gene-edited HSPCs to a fully developed leukemia phenotype in vivo supports the hypothesis, based on clinical and genomic observations, that MLL fusion genes require fewer cooperating oncogenic events for leukemic transformation than other fusion oncoproteins.[5,7] This is consistent with MLL rearrangements

Downloaded from http://ashpublications.net/blood/article-pdf/126/14/1683/1389098/1683.pdf by guest on 20 May 2024

that arise in utero in the majority of infants with acute leukemia, and are unique in their ability to produce overt clinical disease within a few months.[59,60] Preliminary analyses suggest that our leukemias lack mutations in candidate driver genes KRAS, NRAS, FLT3, and PIK3CA[7] when assessed using previously published primers.[61,62] However, these studies were not exhaustive and in the future, our model system can be used to further elucidate the pivotal role of secondary mutations in MLL-rearranged leukemogenesis and provide an experimental platform to further investigate driver and passenger mutations. It promises potential insights into the early events of MLL fusion-driven leukemogenesis and allows for further prospective studies of leukemia initiation and stem cell biology.

Acknowledgments

The authors thank Dan Voytas (University of Minnesota) for generously providing the TALEN Golden Gate library, and Daniel E. Vega Salazar (Stanford Hospital) for his efforts and assistance in the collection of huCB.

This work was supported in part by grants from the National Institutes of Health, National Cancer Institute grants CA116606 and CA160384 (M.L.C.), Alex's Lemonade Stand Foundation (M.L.C.), Hyundai Hope on Wheels (M.P.), the Dr. Mildred Scheel Stiftung (C.B., D.S.), the St. Baldrick's Foundation (E.H.B.), and the German Research Foundation (Deutsche Forschungsgemeinschaft, ref. DU128712-1; J.D.).

Authorship

Contribution: C.B. designed and performed the research, analyzed data, and wrote the manuscript; E.H.B., D.S., J.J., C.-H.L., J.D.-A., S.H.K.W., and K.S.S. performed research and analyzed data; R.S.N. provided patient material; M.P. provided fruitful discussions and guidance; M.L.C. provided overall guidance; and all authors edited the manuscript for content.

Conflict-of-interest disclosure: The authors declare no competing financial interests.

Correspondence: Michael L. Cleary, Lokey Stem Cell Research Building, Room G2034, 1291 Welch Rd, Stanford, CA 94305; e-mail: mcleary@stanford.edu.

References

1. Daser A, Rabbitts TH. Extending the repertoire of the mixed-lineage leukemia gene MLL in leukemogenesis. *Genes Dev.* 2004;18(9): 965-974.
2. Dimartino JF, Cleary ML. Mll rearrangements in haematological malignancies: lessons from clinical and biological studies. *Br J Haematol.* 1999;106(3):614-626.
3. De Braekeleer M, Morel F, Le Bris MJ, Herry A, Douet-Guilbert N. The MLL gene and translocations involving chromosomal band 11q23 in acute leukemia. *Anticancer Res.* 2005;25(3B): 1931-1944.
4. Rubnitz JE, Onciu M, Pounds S, et al. Acute mixed lineage leukemia in children: the experience of St Jude Children's Research Hospital. *Blood.* 2009;113(21):5083-5089.
5. Cancer Genome Atlas Research Network. Genomic and epigenomic landscapes of adult de novo acute myeloid leukemia [published correction appears in *N Engl J Med.* 2013;369(1): 98]. *N Engl J Med.* 2013;368(22):2059-2074.
6. Eguchi M, Eguchi-Ishimae M, Greaves M. The role of the MLL gene in infant leukemia. *Int J Hematol.* 2003;78(5):390-401.
7. Andersson AK, Ma J, Wang J, et al; St. Jude Children's Research Hospital–Washington University Pediatric Cancer Genome Project. The landscape of somatic mutations in infant MLL-rearranged acute lymphoblastic leukemias. *Nat Genet.* 2015;47(4):330-337.
8. Kong CT, Sham MH, So CW, Cheah KS, Chen SJ, Chan LC. The Mll-Een knockin fusion gene enhances proliferation of myeloid progenitors derived from mouse embryonic stem cells and causes myeloid leukaemia in chimeric mice. *Leukemia.* 2006;20(10):1829-1839.
9. Corral J, Lavenir I, Impey H, et al. An Mll-AF9 fusion gene made by homologous recombination causes acute leukemia in chimeric mice: a method to create fusion oncogenes. *Cell.* 1996;85(6):853-861.
10. Chen W, Li Q, Hudson WA, Kumar A, Kirchhof N, Kersey JH. A murine Mll-AF4 knock-in model results in lymphoid and myeloid deregulation and hematologic malignancy. *Blood.* 2006;108(2): 669-677.
11. Doyon Y, Vo TD, Mendel MC, et al. Enhancing zinc-finger-nuclease activity with improved obligate heterodimeric architectures. *Nat Methods.* 2011;8(1):74-79.
12. Genovese P, Schiroli G, Escobar G, et al. Targeted genome editing in human repopulating haematopoietic stem cells. *Nature.* 2014; 510(7504):235-240.
13. Joung JK, Sander JD. TALENs: a widely applicable technology for targeted genome editing. *Nat Rev Mol Cell Biol.* 2013;14(1):49-55.
14. Sander JD, Joung JK. CRISPR-Cas systems for editing, regulating and targeting genomes. *Nat Biotechnol.* 2014;32(4):347-355.
15. Heckl D, Kowalczyk MS, Yudovich D, et al. Generation of mouse models of myeloid malignancy with combinatorial genetic lesions using CRISPR-Cas9 genome editing. *Nat Biotechnol.* 2014;32(9):941-946.
16. Haferlach T, Kohlmann A, Wieczorek L, et al. Clinical utility of microarray-based gene expression profiling in the diagnosis and subclassification of leukemia: report from the International Microarray Innovations in Leukemia Study Group. *J Clin Oncol.* 2010;28(15): 2529-2537.
17. Meyer C, Hofmann J, Burmeister T, et al. The MLL recombinome of acute leukemias in 2013. *Leukemia.* 2013;27(11):2165-2176.
18. Doyle EL, Booher NJ, Standage DS, et al. TAL effector-nucleotide targeter (TALE-NT) 2.0: tools for TAL effector design and target prediction. *Nucleic Acids Res.* 2012;40(Web Server issue): W117-W122.
19. Cermak T, Doyle EL, Christian M, et al. Efficient design and assembly of custom TALEN and other TAL effector-based constructs for DNA targeting [*Nucleic Acids Res.* 2011;39(17):7879]. *Nucleic Acids Res.* 2011;39(12):e82.
20. Breese EH, Buechele C, Dawson C, et al. Use of genome engineering to create patient specific MLL translocations in primary human hematopoietic stem and progenitor cells. *PLoS One.* 2015;10(9):e0136644.
21. Brinkman EK, Chen T, Amendola M, van Steensel B. Easy quantitative assessment of genome editing by sequence trace decomposition. *Nucleic Acids Res.* 2014;42(22):e168.
22. Shaner NC, Lambert GG, Chammas A, et al. A bright monomeric green fluorescent protein derived from Branchiostoma lanceolatum. *Nat Methods.* 2013;10(5):407-409.
23. Somervaille TC, Cleary ML. Identification and characterization of leukemia stem cells in murine MLL-AF9 acute myeloid leukemia. *Cancer Cell.* 2006;10(4):257-268.
24. Lavau C, Szilvassy SJ, Slany R, Cleary ML. Immortalization and leukemic transformation of a myelomonocytic precursor by retrovirally transduced HRX-ENL. *EMBO J.* 1997;16(14): 4226-4237.
25. Qiu P, Shandilya H, D'Alessio JM, O'Connor K, Durocher J, Gerard GF. Mutation detection using Surveyor nuclease. *Biotechniques.* 2004;36(4): 702-707.
26. Ciccia A, Elledge SJ. The DNA damage response: making it safe to play with knives. *Mol Cell.* 2010; 40(2):179-204.
27. Langer T, Metzler M, Reinhardt D, et al. Analysis of t(9;11) chromosomal breakpoint sequences in childhood acute leukemia: almost identical MLL breakpoints in therapy-related AML after treatment without etoposides. *Genes Chromosomes Cancer.* 2003;36(4):393-401.
28. Atlas M, Head D, Behm F, et al. Cloning and sequence analysis of four t(9;11) therapy-related leukemia breakpoints. *Leukemia.* 1998;12(12): 1895-1902.
29. Fu JF, Liang DC, Shih LY. Analysis of acute leukemias with MLL/ENL fusion transcripts: identification of two novel breakpoints in ENL. *Am J Clin Pathol.* 2007;127(1):24-30.
30. Rubnitz JE, Behm FG, Curcio-Brint AM, et al. Molecular analysis of t(11;19) breakpoints in childhood acute leukemias. *Blood.* 1996;87(11): 4804-4808.
31. Elia L, Grammatico S, Paoloni F, et al. Clinical outcome and monitoring of minimal residual disease in patients with acute lymphoblastic leukemia expressing the MLL/ENL fusion gene. *Am J Hematol.* 2011;86(12):993-997.

Downloaded from http://ashpublications.net/blood/article-pdf/126/14/1683/1389098/1683.pdf by guest on 20 May 2024

32. Barabé F, Kennedy JA, Hope KJ, Dick JE. Modeling the initiation and progression of human acute leukemia in mice. *Science.* 2007;316(5824): 600-604.
33. Wei J, Wunderlich M, Fox C, et al. Microenvironment determines lineage fate in a human model of MLL-AF9 leukemia. *Cancer Cell.* 2008;13(6):483-495.
34. Guenther MG, Lawton LN, Rozovskaia T, et al. Aberrant chromatin at genes encoding stem cell regulators in human mixed-lineage leukemia. *Genes Dev.* 2008;22(24):3403-3408.
35. Krivtsov AV, Feng Z, Lemieux ME, et al. H3K79 methylation profiles define murine and human MLL-AF4 leukemias. *Cancer Cell.* 2008;14(5): 355-368.
36. Milne TA, Martin ME, Brock HW, Slany RK, Hess JL. Leukemogenic MLL fusion proteins bind across a broad region of the Hox a9 locus, promoting transcription and multiple histone modifications. *Cancer Res.* 2005;65(24): 11367-11374.
37. Monroe SC, Jo SY, Sanders DS, et al. MLL-AF9 and MLL-ENL alter the dynamic association of transcriptional regulators with genes critical for leukemia. *Exp Hematol.* 2011;39(1):77-86.
38. Mueller D, García-Cuéllar MP, Bach C, Buhl S, Maethner E, Slany RK. Misguided transcriptional elongation causes mixed lineage leukemia. *PLoS Biol.* 2009;7(11):e1000249.
39. Nguyen AT, Taranova O, He J, Zhang Y. DOT1L, the H3K79 methyltransferase, is required for MLL-AF9-mediated leukemogenesis. *Blood.* 2011;117(25):6912-6922.
40. Okada Y, Feng Q, Lin Y, et al. hDOT1L links histone methylation to leukemogenesis. *Cell.* 2005;121(2):167-178.
41. Thiel AT, Blessington P, Zou T, et al. MLL-AF9-induced leukemogenesis requires coexpression of the wild-type Mll allele. *Cancer Cell.* 2010;17(2): 148-159.
42. Chang MJ, Wu H, Achille NJ, et al. Histone H3 lysine 79 methyltransferase Dot1 is required for immortalization by MLL oncogenes. *Cancer Res.* 2010;70(24):10234-10242.
43. Jo SY, Granowicz EM, Maillard I, Thomas D, Hess JL. Requirement for Dot1l in murine postnatal hematopoiesis and leukemogenesis by MLL translocation. *Blood.* 2011;117(18): 4759-4768.
44. Yokoyama A, Lin M, Naresh A, Kitabayashi I, Cleary ML. A higher-order complex containing AF4 and ENL family proteins with P-TEFb facilitates oncogenic and physiologic MLL-dependent transcription. *Cancer Cell.* 2010;17(2):198-212.
45. Anglin JL, Deng L, Yao Y, et al. Synthesis and structure-activity relationship investigation of adenosine-containing inhibitors of histone methyltransferase DOT1L. *J Med Chem.* 2012; 55(18):8066-8074.
46. Yu W, Chory EJ, Wernimont AK, et al. Catalytic site remodelling of the DOT1L methyltransferase by selective inhibitors. *Nat Commun.* 2012;3: 1288.
47. Daigle SR, Olhava EJ, Therkelsen CA, et al. Selective killing of mixed lineage leukemia cells by a potent small-molecule DOT1L inhibitor. *Cancer Cell.* 2011;20(1):53-65.
48. Daigle SR, Olhava EJ, Therkelsen CA, et al. Potent inhibition of DOT1L as treatment of MLL-fusion leukemia. *Blood.* 2013;122(6):1017-1025.
49. Basavapathruni A, Olhava EJ, Daigle SR, et al. Nonclinical pharmacokinetics and metabolism of EPZ-5676, a novel DOT1L histone methyltransferase inhibitor. *Biopharm Drug Dispos.* 2014;35(4):237-252.
50. Klaus CR, Iwanowicz D, Johnston D, et al. DOT1L inhibitor EPZ-5676 displays synergistic antiproliferative activity in combination with standard of care drugs and hypomethylating agents in MLL-rearranged leukemia cells. *J Pharmacol Exp Ther.* 2014;350(3):646-656.
51. Chen W, O'Sullivan MG, Hudson W, Kersey J. Modeling human infant MLL leukemia in mice: leukemia from fetal liver differs from that originating in postnatal marrow. *Blood.* 2011; 117(12):3474-3475.
52. Moriya K, Suzuki M, Watanabe Y, et al. Development of a multi-step leukemogenesis model of MLL-rearranged leukemia using humanized mice. *PLoS One.* 2012;7(6):e37892.
53. Horton SJ, Huntly BJ. Recent advances in acute myeloid leukemia stem cell biology. *Haematologica.* 2012;97(7):966-974.
54. Chen W, Kumar AR, Hudson WA, et al. Malignant transformation initiated by Mll-AF9: gene dosage and critical target cells. *Cancer Cell.* 2008;13(5): 432-440.
55. Ziemin-van der Poel S, McCabe NR, Gill HJ, et al. Identification of a gene, MLL, that spans the breakpoint in 11q23 translocations associated with human leukemias. *Proc Natl Acad Sci USA.* 1991;88(23):10735-10739.
56. Ayton PM, Cleary ML. Transformation of myeloid progenitors by MLL oncoproteins is dependent on Hoxa7 and Hoxa9. *Genes Dev.* 2003;17(18): 2298-2307.
57. Faber J, Krivtsov AV, Stubbs MC, et al. HOXA9 is required for survival in human MLL-rearranged acute leukemias. *Blood.* 2009;113(11): 2375-2385.
58. Wong P, Iwasaki M, Somervaille TC, So CW, Cleary ML. Meis1 is an essential and rate-limiting regulator of MLL leukemia stem cell potential [published correction appears in *Genes Dev.* 2007;21(22):3017]. *Genes Dev.* 2007;21(21): 2762-2774.
59. Ford AM, Ridge SA, Cabrera ME, et al. In utero rearrangements in the trithorax-related oncogene in infant leukaemias. *Nature.* 1993;363(6427): 358-360.
60. Greaves MF, Maia AT, Wiemels JL, Ford AM. Leukemia in twins: lessons in natural history. *Blood.* 2003;102(7):2321-2333.
61. Paulsson K, Horvat A, Strömbeck B, et al. Mutations of FLT3, NRAS, KRAS, and PTPN11 are frequent and possibly mutually exclusive in high hyperdiploid childhood acute lymphoblastic leukemia. *Genes Chromosomes Cancer.* 2008; 47(1):26-33.
62. Samuels Y, Wang Z, Bardelli A, et al. High frequency of mutations of the PIK3CA gene in human cancers. *Science.* 2004;304(5670): 554.

Downloaded from http://ashpublications.net/blood/article-pdf/126/14/1683/1389098/1683.pdf by guest on 20 May 2024